doi: 10.18323/2782-4039-2024-1-67-7

On the possibility of local measurement of crack resistance of structural steels taking into account the structure

Maxim I. Sergeyev*, postgraduate student
Egor V. Pogorelov[1], postgraduate student
Artemiy A. Dudarev, graduate student
Elina A. Sokolovskaya[2], PhD (Engineering), Associate Professor,
assistant professor of Chair of Metal Science and Physics of Strength
Aleksandr V. Kudrya, Doctor of Sciences (Engineering), Professor,
professor of Chair of Materials Science and Strength Physics
University of Science and Technology MISIS, Moscow (Russia)

***E-mail: m1600219@edu.misis.ru**

[1]ORCID: https://orcid.org/0000-0002-6768-5038
[2]ORCID: https://orcid.org/0000-0001-9381-9223

Received 27.06.2023 *Accepted 04.03.2024*

Abstract: The scale of heterogeneity of the structures of steels and alloys can be rather large both within one sample and within a product. The procedure adopted in practice for determining the integral values of crack resistance characteristics cannot always reflect this circumstance. In this regard, it is necessary to develop methods for assessing the crack resistance of a medium with a heterogeneous structure. In this work, the authors determined the crack resistance of large forgings made of heat-hardenable 38KhN3MFA-Sh steel (0.38%C–Cr–3%Ni–Mo–V) based on the critical crack opening δ_c and the *J*-integral. The presence of critical stages in the development of a ductile crack during testing was assessed by acoustic emission measurements. In combination with the obtained methods of digital fractography of 3D images of fractures, this allowed relating the shape and position of the leading edge of each crack jump to the load-displacement diagram. Measuring the crack opening geometry during the test showed the possibility of determining directly the coefficient of crack face rotation when estimating δ_c. In general, this allowed constructing a map of the distribution of parameter δ_c values over the thickness of the sample and estimating the scale of the scatter in crack resistance within one sample – up to 30 %. Such a localization of measurements, primarily of the δ_c parameter, is comparable to the scale of heterogeneity in the morphology of various types of structures, which was assessed based on the measurement of digital images of the dendritic structure, the Bauman sulfur print, non-metallic inclusions on an unetched section, and ferrite-pearlite banding in the microstructure. This makes it possible to link local crack resistance values to various fracture mechanisms and their accompanying structural components.

Keywords: heterogeneity of structures; crack resistance; acoustic emission; fractography; quality prediction in metallurgy; critical crack opening; Cherepanov–Rice integral; nonlinear fracture mechanics.

Acknowledgments: The paper was written on the reports of the participants of the XI International School of Physical Materials Science (SPM-2023), Togliatti, September 11–15, 2023.

For citation: Sergeyev M.I., Pogorelov E.V., Dudarev A.A., Sokolovskaya E.A., Kudrya A.V. On the possibility of local measurement of crack resistance of structural steels taking into account the structure. *Frontier Materials & Technologies*, 2024, no. 1, pp. 71–81. DOI: 10.18323/2782-4039-2024-1-67-7.

INTRODUCTION

The production of materials, in particular steels, is characterized by technological heredity – a mechanism for the evolution of structure and defects determined by the technological process trajectory [1; 2]. Within the tolerance limit of standard technology, a wide range of technological process trajectories is usually observed, the implementation of which leads to the formation of various structures in the material, nominally identical, but differing in the geometry of their structure [3; 4]. This is the reason for the scatter in properties, primarily viscosity (material's resistance to crack propagation), often significant [3; 5].

Within the current GOST 25.506-85, BS 7448-Part 1, and ASTM E1290 standards, it is assumed that the force criterion K_{1c} should be determined under the conditions of plane deformation, the deformation criterion – critical crack opening δ_c and the energy criterion – *J*-integral should be determined under conditions of developed plastic deformation and ductile crack undergrowth. All of them give crack resistance values when testing a sample with a pre-induced fatigue crack. It is obvious that in the presence of a heterogeneous structure, the integral value of crack resistance is the result of the "addition" of the crack resistance values of individual structural components, the level of which is determined, among other things, by the size, shape of similar structural elements, and their spatial configuration. In this regard, the determination of crack resistance should provide for the possibility of linking it to the structure, the heterogeneity of its structure, for example, as was implemented within the local assessment of cold brittleness on samples whose dimensions are comparable to the scale of individual structural components [3]. The updating of regulatory documents related to the determination of crack resistance on massive samples has actually maintained the approaches to its assessment proposed several

decades ago. Until recently, the solution to this problem was complicated by difficulties associated with the correct description of the topography of fractures, in particular, its labor intensity, which makes their assessment qualitative [6; 7]. Therefore, for example, it is impossible to identify objectively the positions of the leading front of a growing crack in a fracture at the time of its successive jumps. Understanding this is necessary to identify the patterns of ductile crack propagation kinetics, in particular, in connection with the need to determine the critical stages of its development [7; 8]. Due to the morphology diversity of similar structures, which determines differences in the mechanisms and, consequently, in the crack propagation kinetics, it is not always clear to what extent the use of the maximum load value during testing as a critical value recommended by regulatory documents corresponds to reality [3; 6]. The use of acoustic emission (AE) for this purpose is not always accompanied by a comparison with direct results of measuring the topography of fractures, which complicates the interpretation of the results obtained [9; 10]. It is obvious that the development of digital methods for measuring structures and fractures can allow progressing in this direction, but a number of issues related to their metrological support still remain unresolved, which complicates the assessment of the reproducibility and comparability of the results obtained [3; 11]. However, the consistent development and application of methods for digitalization of measurements in crack resistance tests should provide a deeper understanding of the patterns of crack opening and propagation, which will allow developing refined approaches to determining fracture toughness, including assessing the possibility of linking the results to the structure heterogeneity. This is important for developing justified technology solutions aimed at increasing the consistent quality of metal [3; 5; 12].

The purpose of this work is to clarify the methods for determining criteria for nonlinear fracture mechanics based on measuring the crack geometry and opening, and to assess the possibility of linking crack resistance values to the structure heterogeneity.

METHODS

The metal of large forgings made of heat-hardenable steels of 38KhN3MFA-Sh (0.38%C–Cr–3%Ni–Mo–V) and 15Kh2NMFA (0.15%C–2%Cr–Ni–Mo–V) types with varying degrees of preserved cast structure and 09G2S (0.09%C–2%Mn–Si) sheet steel (Table 1) produced according to current industrial technologies was used as research objects.

Deep etching in a 50 % aqueous HCl solution (for ~30 min), 3 % HNO_3 solution (up to 3–5 s) was used to identify the dendritic structure and microstructure, respectively, and the Bauman method was used to obtain a sulfur print.

Digital images (in 256 shades of gray) of microstructures and non-metallic inclusions (NMI) on unetched sections were obtained using light microscopy (Axio Observer D1m Carl Zeiss class in the magnification range of 50–1000 times). To convert the images of macrostructures and the sulfur print into digital form, the authors also used an AGFA 1280 digital camera with a CCD matrix and a DUOSCAN T1200 scanner at a resolution of 500 dpi (film negatives at a magnification of ×0.5, the sulfur print at the sample scale).

To measure the geometry of structures and fractures, their primary digital 2D images (in 256 shades of gray) were converted into a "1-0" matrix (black and white) based on an analysis of the image brightness field. The illumination unevenness in the field of view was eliminated by subtracting an optimal degree polynomial; noise (not definitely identifiable small objects) was removed by filtration (taking into account the nature of the object's structure, usually ≤5–10 μm^2) [11].

Assessment of the heterogeneity of the placement of dark spots of sulfur prints was carried out by dividing the image into Voronoi polyhedra – polygons, in each of which all points are closer to its center than the points in neighboring polyhedra. In this case, the distribution of distances between neighboring polyhedra will objectively reflect the location of the sulfur print dark spots [3]. The difference in measurement results was assessed based on the nonparametric Smirnov criterion [13].

Digital three-dimensional images of fractures were obtained at the sample scale using the component module for the "Optofract – 5M" optical microscope (Russia), as well as optical units of the MBS-9 microscope (Russia) and a Nikon J1 digital system camera, resolution 10.1 megapixels. The method resolution was 5–10 μm for each of the three coordinates, the total analyzed volume corresponded to the fracture area in plan (taking into account measurements in the third direction) [15].

A digital three-dimensional triangulation model based on the obtained series of photographs was created using the OpenMVG, OpenMVS software packages and specially developed service modules in the C++ and Python programming languages. As a result of software reconstruction of the surface, non-textured triangulation models were obtained in the Stanford PLY and Wavefront OBJ formats. Visualization and editing (surfaces and point clouds) were carried out using MeshLab and CloudCompare software, the main 3D relief characteristics were calculated using Gwyddion software [1].

Fracture toughness tests were carried out using a three-point bending scheme in accordance with the GOST 25.506-85 standard on an Instron 150LX testing machine (USA) using rectangular specimens of type 4 (with dimensions of 15×20×120 mm) with a notch and a pre-grown fatigue crack, at loading speed of not more than 0.2 mm/min at room test temperature.

The force (K_{IC}) and energy (J-integral) crack resistance criteria were assessed in accordance with the GOST 25.506 standard. The value of the critical crack opening δ_c was also determined based on the concept that assumes that crack opening occurs by rotating its edges around a certain center (axis) [15, p. 86]:

$$\delta_c = V_c \frac{1}{1 + n\frac{l+z}{B-l}},$$

where V_c is the sensor displacement at critical load;
l is the crack length;
n is the rotation coefficient;

z is the distance from the displacement sensor location to the sample;
B is the height of the sample.

The coefficient *n* was determined experimentally based on finding the position of the center of rotation of the crack edges along the sample height (*L*) [14]:

$$n_{exp} = \frac{B-l}{L-(l+z)}.$$

The kinetics of stepped crack propagation was studied using the AE method and quantitative analysis of fractures. With a large number $N>>1$ of small AE pulses, informative emission signals corresponding to crack jumps, linked to the "Bending load *(P)* – Displacement *(V)*" diagram, were separated from the cumulative distribution $N(A)$ – the total number of pulses *N* with amplitude less than *A* [16].

The values of the critical crack opening δ_c and the *J*-integral were determined for each of the first crack jumps, δ_c – also for individual points of the leading crack edge.

RESULTS

The presence of different-scale structures in materials, from dendritic patterns of different geometries to microstructures of different morphologies, leads to a significant scatter in properties due to the influence of heterogeneity of structures on fracture mechanisms. Heterogeneity of structures at all scale observation levels was also present in the steels under study. It was observed both within one sample and from sample to sample. For example, a pair-wise comparison of samples of the results of measuring the NMI areas (at least 2000 pieces per option) at a 100-fold increase in four equal areas (not less than 80 mm^2 each) of the surface of an unetched section (total area ~340 mm^2) made of 38KhN3MFA-Sh (0.38%C–Cr–3%Ni–Mo–V) steel based on the Smirnov *D* criterion identified a significant difference with a risk of 0.05 (with a table value of $D_{0.05}$=1.36[1]) (Table 2).

The difference in the criterion experimental values reflects the difference in the statistics of the distribution of non-metallic inclusions areas in the studied parts of the section, which, in turn, is a consequence of the heterogeneity of the forging dendritic structure. This heterogeneity in the geometry of inclusions may be one of the reasons for the scatter in fracture toughness values.

The Bauman sulfur print morphology evidences the existence of NMI heterogeneity of a different scale in the same forgings associated with the presence in their structure of separate dendritic liquation zones (Fig. 1): columnar dendrites reflecting the heat removal direction to the surface of the forging (peripheral zone), a mixture of equiaxial small dendrites in the intermediate zone and coarse equiaxial dendrites in the central one (Fig. 2 a).

For the development of ductile fracture, both the size of sulfides and their placement on the surface of the polished section are important: their close location to each other facilitates the ductile fracture initiation, and an increase in their sparseness promotes the development of plastic deformation. The selection of the nearest neighbors on the plane was obtained based on partitioning the sulfur print image into Voronoi polyhedra (Fig. 2 b, 2 c). Partitioning the image into Voronoi polyhedra showed that the average distances between the centers of the polyhedra for different liquation zones (peripheral, intermediate and central) were close and amounted to 3.70±0.02; 3.70±0.01; 3.39±0.02 mm, respectively. The heterogeneity of the placement of the sulfur print dark spots of the forging of 38KhN3MFA-Sh (0.38%C–Cr–3%Ni–Mo–V) steel is evidenced, in particular, by the distribution of distances between their centers for forging areas corresponding to different zones of liquation (peripheral, intermediate and central) reflecting differences in the dendritic pattern morphology (Table 3).

With a similar distribution of distances between spots in each of the areas of the forgings, as evidenced by the values of the skewness and kurtosis coefficients (Table 4), differences are observed between the samples related to the results of measuring the distances between dark neighboring spots. This may be one of the reasons for the scatter of properties over the forging cross-section. The reason for such heterogeneity in the distribution of sulfides (sulfur print dark spots) was most likely liquation. A comparison of samples – the results of measuring the pitch of dendrites, for example, in the central and intermediate regions of the forging according to the Smirnov criterion, revealed their significant difference (D_{exp}=1.121 > $D_{0.118}$=1.19)[2]. The dendrite pitch varied from 60 to 3820 μm.

The remote consequences of liquation were also reflected in the microstructure of 38KhN3MFA-Sh (0.38%C–Cr–3%Ni–Mo–V) steel (a mixture of ferrite and bainite), in which large ferrite areas were observed. Their diameter varied from 95 to 386 μm.

The presence of a dendritic structure in forgings made of 15Kh2NMFA (0.15%C–2%Cr–Ni–Mo–V) steel also contributed to the formation of uneven distribution of sulfur print dark spots and the appearance of different grain sizes in the structure. Etching of samples selected at random revealed austenite grains in the structure differing in the range of maximum diameter *D* values ($\Delta=D_{max}-D_{min}$): 250 and 90 μm, respectively.

Heterogeneity of microstructures is characteristic not only of steels with a remained cast structure – its remote consequences can be observed, for example, in rolled products. The result of this may be differences in the scale of banding in the microstructure over the cross section of an impact sample made of sheet 09G2S (0.09%C–2%Mn–Si) steel (Fig. 3). Comparison of samples of the results of measuring the pitch of pearlite bands in two fields cut out from a panoramic image (along the cross section of an impact sample) using the Smirnov criterion showed that they differ with a risk of 0.05 (D_{exp}=1.37 > $D_{0.05}$=1.36).

Thus, it is obvious that the scale of heterogeneity of different-scale structures can be very large; this is typical when producing the materials, primarily the most widespread – steels. In this regard, assessing the viscosity of a medium with a heterogeneous structure, which allows

[1] *Bolshev L.N., Smirnov N.V. Mathematical Statistics Tables. Nauka, 1965. 464 p.*

[2] *See 1.*

Table 1. *Chemical compositions of steels under study*
Таблица 1. *Химические составы исследуемых сталей*

Steel	Weight fraction of elements, %									
	C	**Mn**	**Si**	**P**	**S**	**Cr**	**Ni**	**Mo**	**V**	**Cu**
38KhN3MFA (0.38%C–Cr–3%Ni–Mo–V)	0.41	0.22	0.22	0.02	0.02	0.87	3.32	0.58	0.14	0.03
09G2S (0.09%C–2%Mn–Si)	0.12	1.3	0.5	0.04	0.04	0.3	0.3	–	–	0.3
15Kh2NMFA (0.15%C–2%Cr–Ni–Mo–V)	0.13	0.3	0.17	0.02	0.02	1.8	1.0	0.5	0.01	0.03

Table 2. *Experimental values of the Smirnov criterion when comparing the results of measuring non-metallic inclusions areas on four equal-area sections of 38KhN3MFA-Sh (0.38%C–Cr–3%Ni–Mo–V) steel*
Таблица 2. *Экспериментальные значения критерия Смирнова при сравнении результатов измерения площадей неметаллических включений на четырех равных по площади участках шлифа из стали 38ХН3МФА-Ш (0,38%C–Cr–3%Ni–Mo–V)*

Panorama section	1	2	3	4
1	–	5.57	2.52	1.85
2	5.57	–	7.18	4.39
3	2.52	7.18	–	3.28
4	1.85	4.39	3.28	–

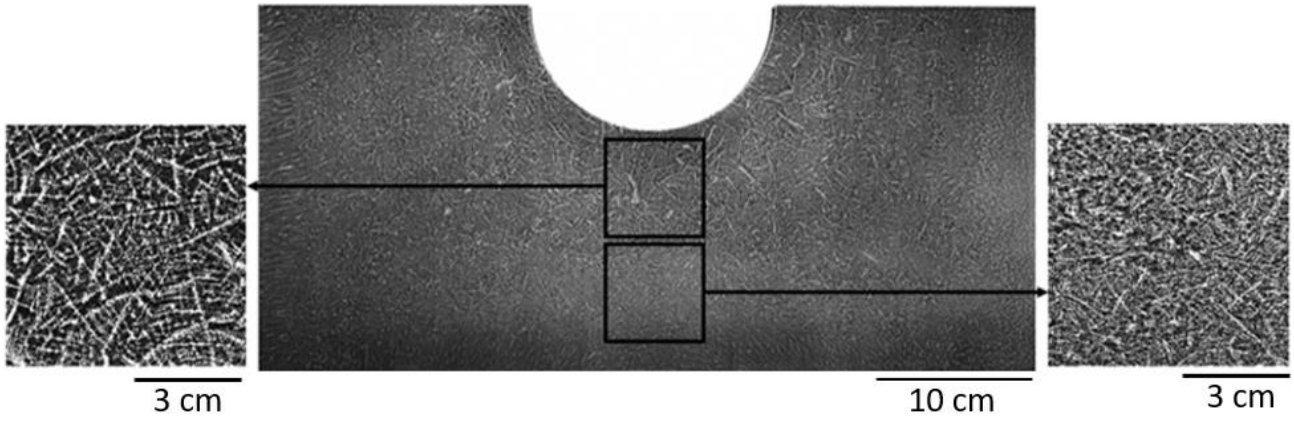

Fig. 1. *Morphology of the dendritic pattern of forging made of 38KhN3MFA-Sh (0.38%C–Cr–3%Ni–Mo–V) steel and its structure in the central and intermediate regions of the forging*
Рис. 1. *Морфология дендритного рисунка поковки из стали 38ХН3МФА-Ш (0,38%C–Cr–3%Ni–Mo–V) и его строение в центральной и промежуточной областях поковки*

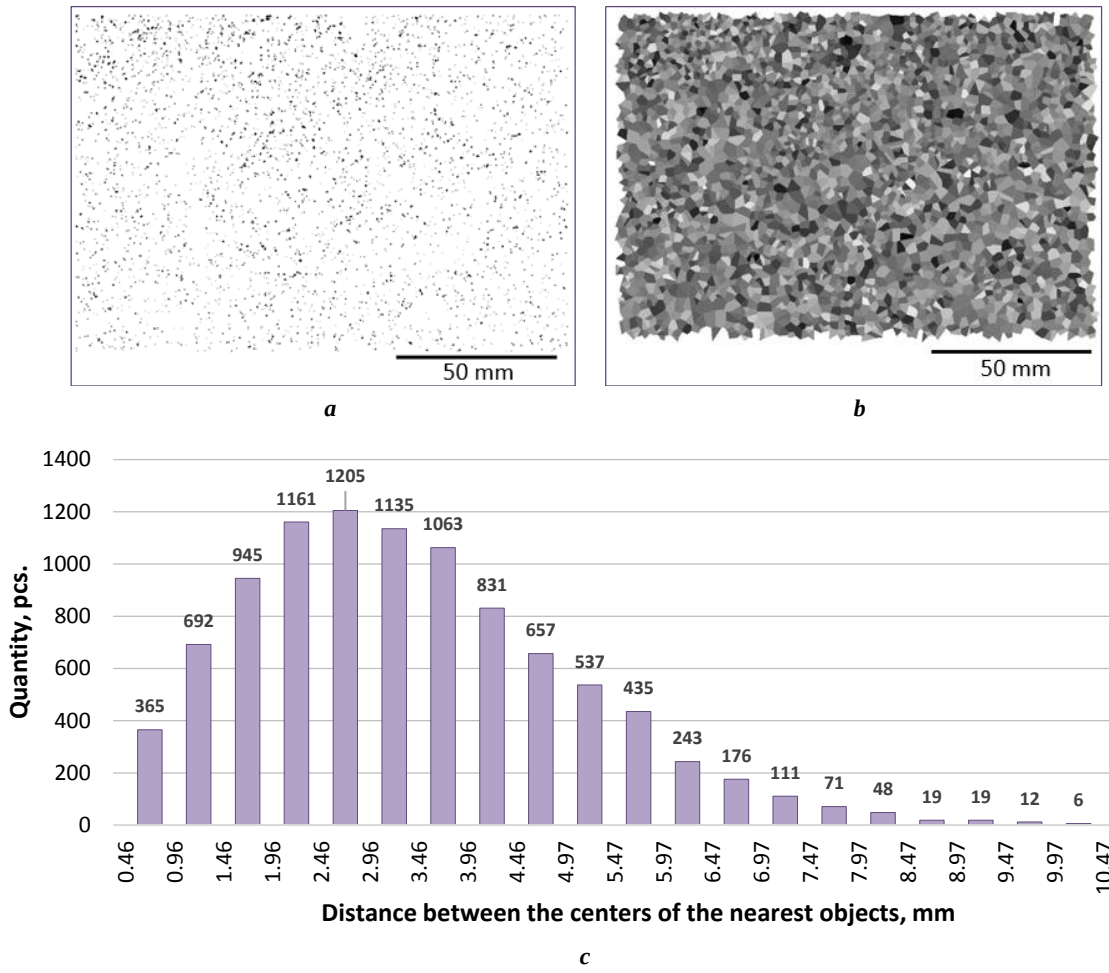

Fig. 2. *Sulfur print image decomposition (**a**) into Voronoi polyhedra (**b**) using the example of the central region of a forging made of tempered 38KhN3MFA-Sh steel (0.38% C–Cr–3% Ni–Mo–V) and the distribution of distances between the centers of gravity of the nearest dark spots (**c**)*

Рис. 2. *Разбиение изображения серного отпечатка (**a**) на полиэдры Вороного (**b**) на примере центральной области поковки из улучшаемой стали 38ХН3МФА-Ш (0,38%C–Cr–3%Ni–Mo–V) и распределение расстояний между центрами тяжести ближайших темных пятен (**c**)*

Table 3. *Experimental values of the Smirnov criterion obtained when comparing the distribution of the number of the nearest dark neighbor spots and the distances between their centers for different fragments of the sulfur print image of the forging made of 38KhN3MFA-Sh (0.38%C–Cr–3%Ni–Mo–V) steel*

Таблица 3. *Экспериментальные значения критерия Смирнова, полученные при сравнении распределений числа ближайших темных пятен-соседей и расстояний между их центрами, для различных фрагментов изображения серного отпечатка поковки из стали 38ХН3МФА-Ш (0,38%C–Cr–3%Ni–Mo–V)*

Forging area under study	Peripheral	Central	Intermediate
Peripheral	–	0.724 (0.6) 7.361 (0.05)	0.629 (0.8) 2.307 (0.05)
Central	0.724 (0.6) 7.361 (0.05)	–	0.588 (0.9) 9.356 (0.05)
Intermediate	0.629 (0.8) 2.307 (0.05)	0.588 (0.9) 9.356 (0.05)	–

Note. The numerator and denominator indicate the experimental values of the Smirnov criterion for the distribution of the number of the nearest dark spots of the sulfur print and the distance between their centers, respectively. The risks of the hypothesis about their differences are indicated in parentheses.

Примечание. В числителе и знаменателе указаны экспериментальные значения критерия Смирнова для распределения числа ближайших темных пятен серного отпечатка и расстояния между их центрами соответственно. В скобках указаны риски гипотезы об их отличии.

Table 4. *Values of the coefficients of skewness and kurtosis of the distributions of the number of neighbors of the nearest sulfur print dark spots and the distances between them in different areas along the cross-section of a forging made of 38KhN3MFA-Sh (0.38%C–Cr–3%Ni–Mo–V) steel*

Таблица 4. *Значения коэффициентов асимметрии и эксцесса распределений числа соседей ближайших темных пятен серного отпечатка и расстояний между ними в различных областях по сечению поковки из стали 38ХН3МФА-Ш (0,38%C–Cr–3%Ni–Mo–V)*

Parameter	Coefficient of	Peripheral region	Central region	Intermediate region
Number of neighbors	skewness	0.456	0.329	0.410
	kurtosis	0.167	−0.045	0.183
Distance between the centers of the nearest dark spots of sulfur print	skewness	0.719	0.737	0.674
	kurtosis	0.421	0.518	0.379

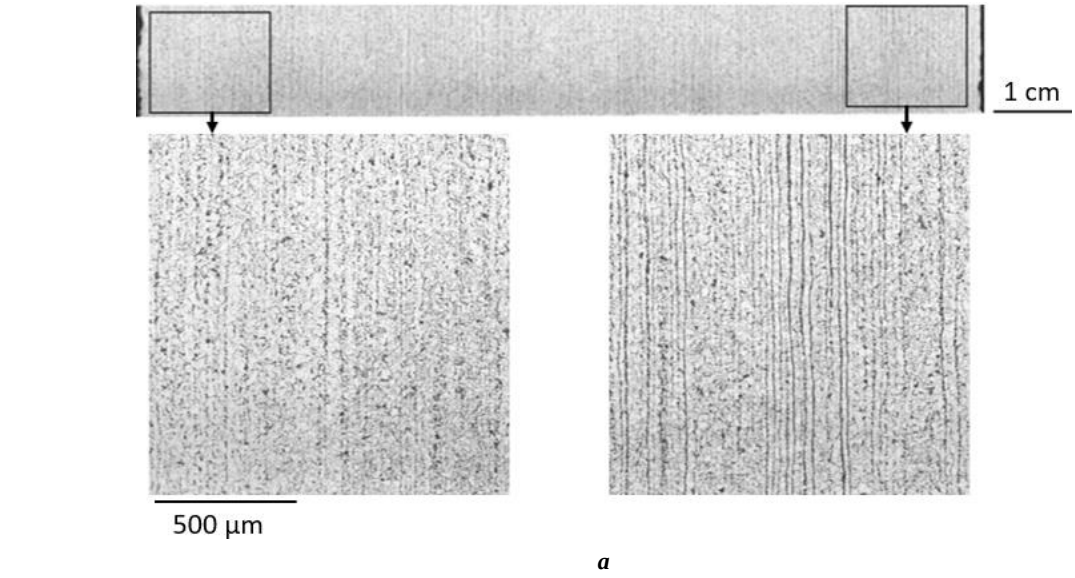

a

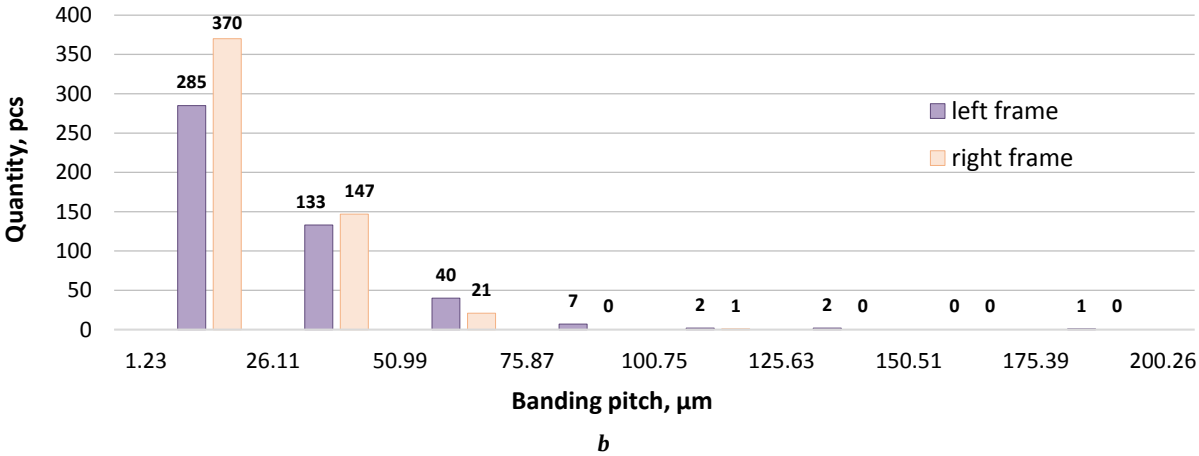

b

Fig. 3. *The observed difference in the scale of banding in the microstructure along the cross-section of an impact sample made of sheet 09G2S (0.09%C–2%Mn–Si) steel in the panorama as a whole and in its different sections (left and right) (**a**) and the corresponding distribution of values of a pitch of perlite strips (**b**)*

Рис. 3. *Наблюдаемое различие в масштабах полосчатости в микроструктуре по сечению ударного образца из листовой стали 09Г2С (0,09%C–2%Mn–Si) на панораме в целом и на отдельных ее участках (левом и правом) (**а**) и соответствующее им распределение значений шага полос перлита (**b**)*

determining the influence of heterogeneity on the fracture resistance, becomes relevant.

When determining fracture toughness based on the *J*-integral and δ_c, the authors assessed the crack propagation kinetics using AE, which made it possible to record pulses during the fracture process (Fig. 4 a). Most of the recorded pulses were of a noise nature. Filtering of AE signals allowed separating signals corresponding to crack jumps (with reference to the "*P* – *V*" diagram, Fig. 4 b).

The obtained results allowed identifying the scale of differences in crack resistance values (critical crack opening) both within each sample and from forging to forging, including the result of crack resistance calculation according to GOST: $\Delta^{\delta c}=\delta_c^{max}-\delta_c^{min}$; $\Delta_1^{\delta c}=|\delta_c^{GOST}-\delta_{c1}|$; $\Delta_{max}^{\delta c}=|\delta_c^{GOST}-\delta_c^{max}|$; $\Delta_{min}^{\delta c}=|\delta_c^{GOST}-\delta_c^{min}|$ (Table 5).

The difference between the δ_c values calculated in accordance with GOST within one sample compared to the CCO value determined experimentally (δ_c^{max}) varied from 3 to 40 % for 38KhN3MFA-Sh (0.38%C–Cr–3%Ni–Mo–V) steel, from 15 to 17 % for 15Kh2NMFA (0.15%C–2%Cr–Ni–Mo–V) steel; it reached 22 and 43 %, respectively, compared to the δ_c^{min} minimum opening value.

The *J*-integral values were also determined for each of the first five crack jumps, taking into account its undergrowth. The obtained results allowed identifying the scale of differences in the *J*-integral values both within each sample and from sample to sample, including with GOST: $\Delta^J=J^{max}-J^{min}$; $\Delta_1^J=|J^{GOST}-J_1|$; $\Delta_{max}^J=|J^{GOST}-J^{max}|$; $\Delta_{max}^J=|J^{GOST}-J^{max}|$; $\Delta_{min}^J=|J^{GOST}-J^{min}|$ (Table 6).

To assess the crack resistance heterogeneity over the sample section, a map of the distribution of critical crack opening values for the second – fourth jumps along the contours of the crack leading edge was compiled (Fig. 5). The first jump from a fatigue crack was not taken into account, since the fracture relief was measured only at the stage of static crack undergrowth.

Therefore, the use of a refined technique for local assessment of the critical crack opening allowed determining the values of crack resistance δ_c over the cross section of the sample.

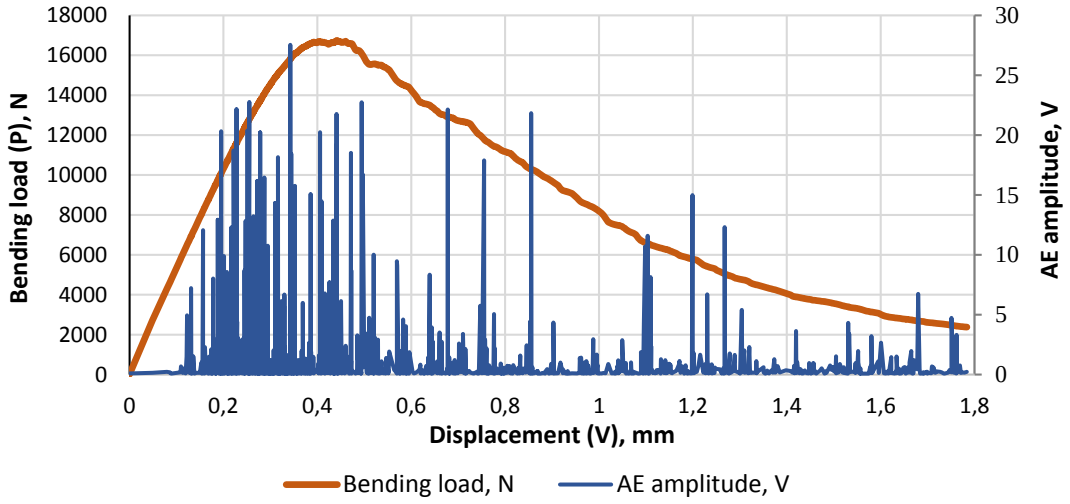

a

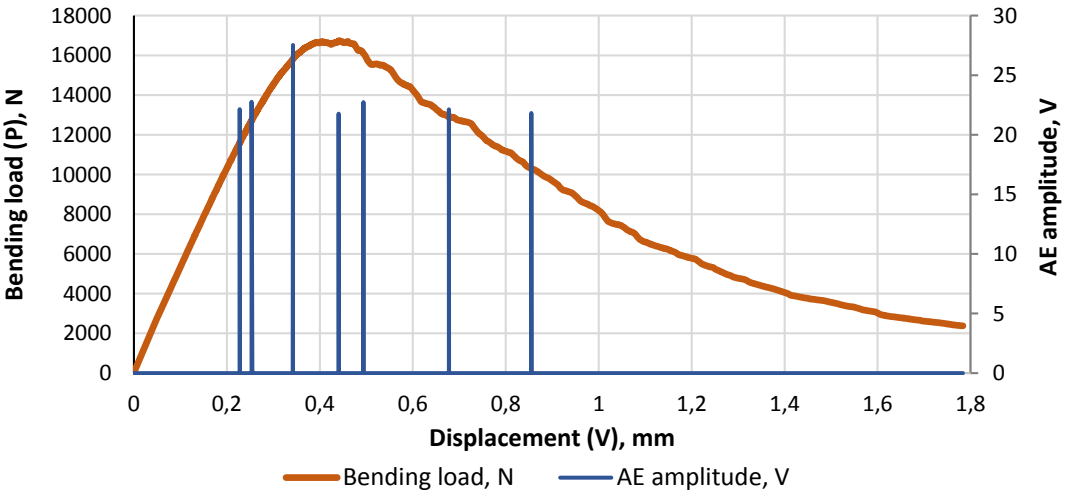

b

Fig. 4. *Loading – displacement diagram and AE signals during the destruction of a sample made of 38KhN3MFA-Sh (0.38%C–Cr–3%Ni–Mo–V) steel before (**a**) and after (**b**) filtration*
Рис. 4. *Диаграмма «нагрузка – смещение» и сигналы АЭ при разрушении образца из стали 38ХН3МФА-Ш (0,38%C–Cr–3%Ni–Mo–V) до (**а**) и после (**b**) фильтрации*

Table 5. *Scale of heterogeneity of δ_c values (mm) of metal forgings with a heterogeneous structure made of 38KhN3MFA-Sh (0.38%C–Cr–3%Ni–Mo–V) and 15Kh2NMFA (0.15%C–2%Cr–Ni–Mo–V) steels*
Таблица 5. *Масштаб неоднородности значений δ_c (мм) металла поковок с неоднородной структурой из стали 38ХН3МФА-Ш (0,38%C–Cr–3%Ni–Mo–V) и 15Х2НМФА (0,15%C–2%Cr–Ni–Mo–V)*

Steel	Sample number	$\Delta_1^{\delta c}$	$\delta_c^{\max}$	$\delta_c^{\min}$	$\Delta^{\delta c}$	$\Delta_{\max}^{\delta c}$	$\Delta_{\min}^{\delta c}$
38KhN3MFA-Sh (0.38%C–Cr–3%Ni–Mo–V)	1	0.005	0.108	0.079	0.029	0.031	0.002
	2	0.016	0.098	0.077	0.021	0.016	0.005
	3	0.031	0.121	0.091	0.030	0.031	0.001
	4	0.002	0.065	0.052	0.013	0.002	0.015
	5	0.007	0.093	0.068	0.025	0.007	0.018
15Kh2NMFA (0,15%C–2%Cr–Ni–Mo–V)	6	0.023	0.347	0.298	0.049	0.051	0.002
	7	0.089	0.228	0.152	0.076	0.040	0.116

Table 6. *Scale of heterogeneity of J-интеграла values (MJ/m^2) of 38KhN3MFA-Sh (0.38%C–Cr–3%Ni–Mo–V) and 15Kh2NMFA (0.15%C–2%Cr–Ni–Mo–V) steels*
Таблица 6. *Масштаб неоднородности значений J-интеграла (МДж/м^2) сталей 38ХН3МФА-Ш (0,38%C–Cr–3%Ni–Mo–V) и 15Х2НМФА (0,15%C–2%Cr–Ni–Mo–V)*

Steel	Sample number	J_{GOST}	$J_{\max}$	$J_{\min}$	Δ^J	Δ_1^J	$\Delta_{\max}^J$	$\Delta_{\min}^J$
38KhN3MFA-Sh (0.38%C–Cr–3%Ni–Mo–V)	1	0.057	0.097	0.066	0.031	0.009	0.040	0.009
	2	0.099	0.081	0.047	0.034	0.044	0.018	0.052
	3	0.070	0.135	0.083	0.052	0.025	0.065	0.013
	4	0.062	0.102	0.079	0.023	0.026	0.040	0.017
	5	0.067	0.064	0.039	0.025	0.028	0.003	0.028
15Kh2NMFA (0,15%C–2%Cr–Ni–Mo–V)	6	0.298	0.587	0.336	0.251	0.038	0.289	0.038
	7	0.274	0.189	0.122	0.067	0.106	0.085	0.152

DISCUSSION

The observed difference in crack resistance values within one sample and between samples showed that taking into account crack undergrowth, including shape restoration of its leading edge (according to AE measurements and fracture topography), provides a wider range of crack resistance values, both the critical crack opening δ_c and the Cherepanov–Rice integral (compared to GOST 25.506). This is significant, since for large forgings made of heat-hardenable 38KhN3MFA-Sh (0.38%C–Cr–3%Ni–Mo–V) and 15Kh2NMFA (0.15%C–2%Cr–Ni–Mo–V) steels, it was shown that the δ_c values within one sample varied from 25 to 37 % and from 16 to 50 %, respectively. At the same time, the values determined in accordance with GOST 25.506 differed from 3 to 34 % for 38KhN3MFA-Sh (0.38%C–Cr–3%Ni–Mo–V) steel and from 8 to 33 % for 15Kh2NMFA (0.15%C–2%Cr–Ni–Mo–V) steel compared to the δ_c values characteristic of the first static crack jump (according to AE measurements).

The *J*-integral value gives the integral value of the fracture energy for each crack jump. It was shown that the *J*-integral values within one sample varied from 29 to 72 % and from 55 to 75 %, respectively. The study revealed a significant difference between the values of the Cherepanov–Rice

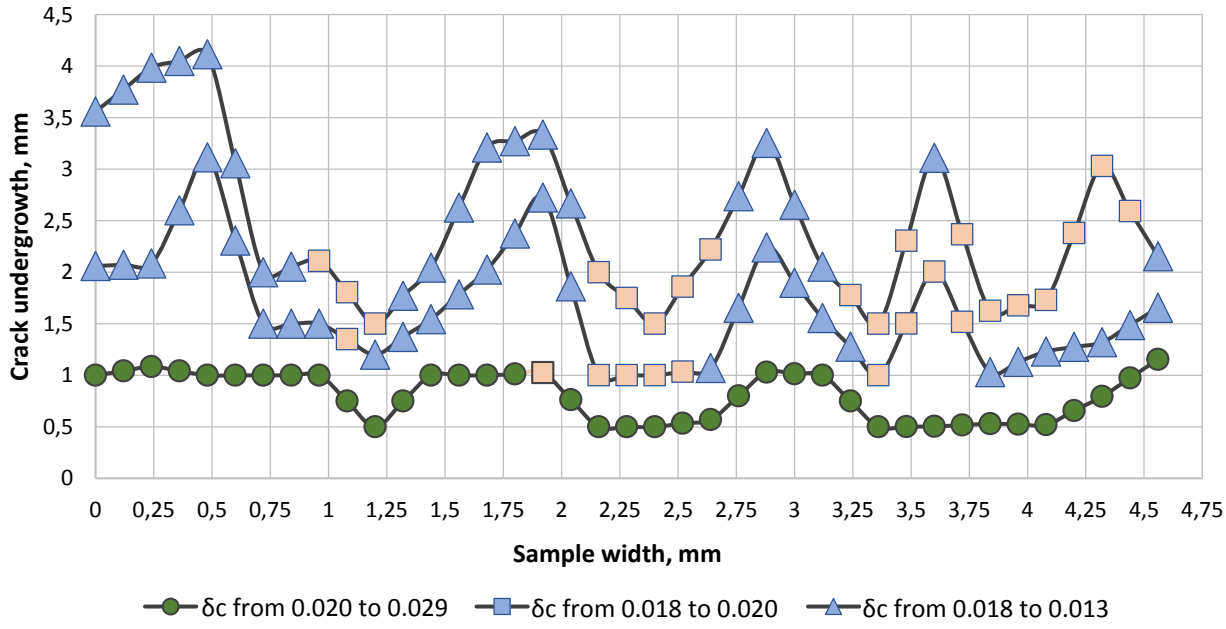

Fig. 5. *Map of the heterogeneity of crack resistance distribution (δ_c values) based on measurements at the bottom of a macrobrittle square for the second – fourth jumps of a ductile crack (the first jump from a fatigue crack was not taken into account), 38KhN3MFA-Sh (0.38%C–Cr–3%Ni–Mo–V)*
Рис. 5. *Карта неоднородности распределения трещиностойкости (значений δ_c) по измерениям на дне макрохрупкого квадрата для второго – четвертого скачков вязкой трещины (первый скачок от усталостной трещины не учитывался), сталь 38ХН3МФА-Ш (0,38%C–Cr–3%Ni–Mo–V)*

integral determined in accordance with GOST 25.506 and the *J*-integral values characteristic of the first static crack jump (according to AE measurements). It was 16–44 % for 38KhN3MFA-Sh (0.38%C–Cr–3%Ni–Mo–V) steel, 13–39 % for 15Kh2NMFA (0.15%C–2%Cr–Ni–Mo–V) steel. This means that using maximum load values as critical values when determining fracture toughness is not always valid.

It is important to note that critical crack opening has the advantage of being able to actually pinpoint the crack opening within each of the leading edges of a growing crack (taking into account their curvature and irregular shape). Hence, the possibility of linking δ_c values to one or another destruction mechanism, which is determined by the type of structure or the features of its local structure. This is important when identifying the causes of the scatter in viscosity, determining its structural and metallurgical factors, and it will allow improving the objectivity of the prediction of metal destruction as a whole. Identifying critical elements of structures is also necessary for managing the quality of metal products, including in real time, changing from selecting structures for given properties to designing structures of optimal configuration [17; 18].

CONCLUSIONS

Direct measurements of images of heterogeneous structures in large forgings made of 38KhN3MFA-Sh (0.38%C–Cr–3%Ni–Mo–V), 15Kh2NMFA (0.15%C–2%Cr–Ni–Mo–V) steels and sheet of 09G2S (0.09%C–2%Mn–Si) steel were used to assess the degree of heterogeneity of their structure, the scale of which should definitely be taken into account when determining their crack resistance. The boundaries of effective application of the criteria of nonlinear fracture mechanics are compared: deformation criterion – critical crack opening δ_c and energy criterion – *J*-integral. The study showed that, in the case the geometry and kinetics of ductile crack development are measured during fracture toughness testing, it is possible to expand the range of values of crack resistance characteristics (for each crack jump on one sample), which is essential for a more complete description of the viscosity reserve of a medium with a heterogeneous structure. The advantage of critical crack opening δ_c – the possibility of relating crack resistance values to the structure – has been identified when assessing structural steels with different-scale structural heterogeneity.

REFERENCES

1. Shtremel M.A. *Razrushenie. Razrushenie materiala* [Destruction. Rupture of material]. Moscow, MISiS Publ., 2015. Kn. 1, 975 p.
2. Shtremel M.A. *Razrushenie. Razrushenie struktur* [Destruction. Rupture of structures]. Moscow, MISiS Publ., 2015. Kn. 2, 975 p.
3. Kudrya A.V., Sokolovskaya E.A., Tang V.F. Possibility of predicting the destruction of metal materials with a heterogeneous structure. *Russian metallurgy (Metally)*, 2022, vol. 2022, no. 10, pp. 1318–1331. DOI: 10.1134/S0036029522100160.
4. Kazakov A.A., Kiselev D.V., Kazakova E.I. Quantitative methods for assessing the microstructure of steel

and alloys for revising outdated GOST standards. *Lite i metallurgiya*, 2021, no. 2, pp. 42–48. DOI: 10.21122/1683-6065-2021-2-42-48.
5. Kudrya A.V., Nikulin S.A., Nikolaev Y.A., Arsenkin A.M., Sokolovskaya E.A., Skorodumov S.V., Chernobaeva A.A., Kuzko E.I., Khoreva E.G. Nonuniformity of the ductility of 15X2HMFA low-alloy steel. *Steel in Translation*, 2009, vol. 39, no. 9, pp. 742–747. EDN: QCKREZ.
6. Tan Long, Li Songyang, Zhao Liangyin, Wang Lulu, Zhao Xiuxiu. The effect of mechanical inhomogeneity in microzones of welded joints on CTOD fracture toughness of nuclear thick-walled steel. *Nuclear Engineering and Technology*, 2023, vol. 55, no. 11, pp. 4112–4119. DOI: 10.1016/j.net.2023.07.031.
7. Li Ai, Soltangharaei V., Greer B., Bayat M., Ziehl P. Structural health monitoring of stainless-steel nuclear fuel storage canister using acoustic emission. *Developments in the Built Environment*, 2024, vol. 17, article number 100294. DOI: 10.1016/j.dibe.2023.100294.
8. Xu Jie, Sun Tong, Xu Yantao, Han Qinghua. Fracture toughness research of G20Mn5QT cast steel based on the acoustic emission technique. *Construction and Building Materials*, 2020, vol. 230, article number 116904. DOI: 10.1016/j.conbuildmat.2019.116904.
9. Vorontsov V.B., Pershin V.K. Correlation between Acoustic Emission and the Local Structural Restructuring in the Nonequilibrium Aluminum Melt. *Russian Metallurgy (Metally)*, 2020, vol. 2020, no. 2, pp. 92–101. DOI: 10.1134/S0036029520020160.
10. Botvina L.R., Tyutin M.R., Bolotnikov A.I., Petersen T.B. effect of preliminary cycling on the acoustic emission characteristics of structural 15Kh2GMF steel. *Russian Metallurgy (Metally)*, 2021, vol. 2021, no. 1, pp. 32–41. EDN: INTJOA.
11. Sokolovskaya E.A., Kudrya A.V., Kodirov D.F., Sergeev M.I., Budanova E.S., Samoshina M.E. On the reliability of the results of digital measurements of images of structures in metal science. *Metallurg*, 2024, no. 1, pp. 36–39. EDN: DGYMXQ.
12. Makhutov N.A. Evolution of laboratory researches and diagnostics of materials. *Zavodskaya laboratoriya. Diagnostika materialov*, 2022, vol. 88, no. 1-1, pp. 5–13. DOI: 10.26896/1028-6861-2022-88-1-I-5-13.
13. Nikitin Y. *Asymptotic efficiency of nonparametric tests*. New York, Cambridge University Press Publ., 1995. 274 p.
14. Kudrya A.V., Sokolovskaya E.A., Ngo Kh.N., Kuzko E.I., Kotishevskiy G.V. Fracture forecasting of large-size forged pieces with multi-scale structure. *Russian metallurgy (metally)*, 2019, vol. 12, no. 12, pp. 1304–1308. DOI: 10.1134/S0036029519120115.
15. Rabotnov Yu.N., ed. *Novye metody otsenki soprotivleniya metallov khrupkomu razrusheniyu* [New methods for assessing the resistance of metals to brittle fracture]. Moscow, Mir Publ., 1972. 438 p.
16. Khanzhin V.G., Shtremel M.A. Quantitative information on fracture processes obtained by measurement of acoustic emission. *Metal Science and Heat Treatment*, 2009, vol. 51, no. 5-6, pp. 250–255. DOI: 10.1007/s11041-009-9146-4.
17. Shtremel M.A., Karabasova L.V., Chizhikov V.I., Vodeniktov S.I. About optimal alloying of high-vanadium high-speed steel. *Metal Science and Heat Treatment*, 1999, vol. 41, no. 3-4, pp. 146–150. DOI: 10.1007/bf02465798.
18. Shtremel M.L., Belomyttsev M.Yu., Medvedev V.V., Mochalov B.V., Chernukha L.G. The structure and features of composite materials having web structure on the base of NiAl intermetallide. *Izvestiya. Ferrous metallurgy*, 2006, no. 1, pp. 40–44. EDN: HTDWRB.

СПИСОК ЛИТЕРАТУРЫ

1. Штремель М.А. Разрушение. В 2 кн. Кн. 1: Разрушение материала. М.: МИСиС, 2015. 975 с.
2. Штремель М.А. Разрушение. В 2 кн. Кн. 2: Разрушение структур. М.: МИСиС, 2015. 975 с.
3. Кудря А.В., Соколовская Э.А., Танг В.Ф. Возможность прогноза разрушения металлических материалов с неоднородной структурой // Деформация и разрушение материалов. 2022. № 6. С. 2–19. EDN: BSVQQW.
4. Казаков А.А., Киселев Д.В., Казакова Е.И. Количественные методы оценки микроструктуры стали и сплавов для пересмотра устаревших ГОСТ // Литье и металлургия. 2021. № 2. С. 42–48. DOI: 10.21122/1683-6065-2021-2-42-48.
5. Кудря А.В., Никулин С.А., Николаев Ю.А., Арсенкин А.М., Соколовская Э.А., Скородумов С.В., Чернобаева А.А., Кузько Е.И., Хорева Е.Г. Факторы неоднородности вязкости низколегированной стали 15Х2НМФА // Известия высших учебных заведений. Черная металлургия. 2009. № 9. С. 23–28. EDN: QCKREZ.
6. Tan Long, Li Songyang, Zhao Liangyin, Wang Lulu, Zhao Xiuxiu. The effect of mechanical inhomogeneity in microzones of welded joints on CTOD fracture toughness of nuclear thick-walled steel // Nuclear Engineering and Technology. 2023. Vol. 55. № 11. P. 4112–4119. DOI: 10.1016/j.net.2023.07.031.
7. Li Ai, Soltangharaei V., Greer B., Bayat M., Ziehl P. Structural health monitoring of stainless-steel nuclear fuel storage canister using acoustic emission // Developments in the Built Environment. 2024. Vol. 17. Article number 100294. DOI: 10.1016/j.dibe.2023.100294.
8. Xu Jie, Sun Tong, Xu Yantao, Han Qinghua. Fracture toughness research of G20Mn5QT cast steel based on the acoustic emission technique // Construction and Building Materials. 2020. Vol. 230. Article number 116904. DOI: 10.1016/j.conbuildmat.2019.116904.
9. Vorontsov V.B., Pershin V.K. Correlation between Acoustic Emission and the Local Structural Restructuring in the Nonequilibrium Aluminum Melt // Russian Metallurgy (Metally). 2020. Vol. 2020. № 2. P. 92–101. DOI: 10.1134/S0036029520020160.
10. Ботвина Л.Р., Тютин М.Р., Болотников А.И., Петерсен Т.Б. Влияние предварительного циклирования на характеристики акустической эмиссии конструкционной стали 15Х2ГМФ // Металлы. 2021. № 1. С. 32–41. EDN: KYXDHW.
11. Соколовская Э.А., Кудря А.В., Кодиров Д.Ф., Сергеев М.И., Буданова Е.С., Самошина М.Е. О достоверности результатов цифровых измерений изображений структур в металловедении // Металлург. 2024. № 1. С. 36–39. EDN: DGYMXQ.
12. Махутов Н.А. Развитие лабораторных исследований и диагностики материалов // Заводская лаборатория.

Диагностика материалов. 2022. Т. 88. № 1-1. С. 5–13. DOI: 10.26896/1028-6861-2022-88-1-I-5-13.
13. Nikitin Y. Asymptotic efficiency of nonparametric tests. New York: Cambridge University Press, 1995. 274 p.
14. Кудря А.В., Соколовская Э.А., Нго Х.Н., Кузько Е.И., Котишевский Г.В. Прогноз разрушения крупных поковок с неоднородной структурой // Электрометаллургия. 2019. № 6. С. 33–39. EDN: XLIBHK.
15. Новые методы оценки сопротивления металлов хрупкому разрушению / под ред. Ю.Н. Работнова. М.: Мир, 1972. 438 с.
16. Ханжин В.Г., Штремель М.А. Количественная информация о процессах разрушения, получаемая при измерениях акустической эмиссии // Металловедение и термическая обработка металлов. 2009. № 5. С. 53–59. EDN: JTSNZB.
17. Shtremel M.A., Karabasova L.V., Chizhikov V.I., Vodeniktov S.I. About optimal alloying of high-vanadium high-speed steel // Металловедение и термическая обработка металлов. 1999. № 4. С. 16–20. EDN: MPCVSV.
18. Штремель М.Л., Беломытцев М.Ю., Медведев В.В., Мочалов Б.В., Чернуха Л.Г. Структура и свойства композиционных материалов на основе интерметаллида NiAl // Известия высших учебных заведений. Черная металлургия. 2006. № 1. С. 40–44. EDN: HTDWRB.

О возможности локального измерения трещиностойкости конструкционных сталей с привязкой к структуре

Сергеев Максим Иванович*, аспирант
Погорелов Егор Васильевич[1], аспирант
Дударев Артемий Александрович, магистр
Соколовская Элина Александровна[2], кандидат технических наук, доцент,
доцент кафедры металловедения и физики прочности
Кудря Александр Викторович, доктор технических наук, профессор,
профессор кафедры металловедения и физики прочности
Университет науки и технологий МИСИС, Москва (Россия)

***E-mail: m1600219@edu.misis.ru**

[1]ORCID: https://orcid.org/0000-0002-6768-5038
[2]ORCID: https://orcid.org/0000-0001-9381-9223

Поступила в редакцию 27.06.2023 *Принята к публикации 04.03.2024*

Аннотация: Масштаб неоднородности структур сталей и сплавов может быть достаточно велик в пределах как одного образца, так и изделия. Принятая на практике процедура определения интегральных значений характеристик трещиностойкости не всегда может отразить это обстоятельство. В этой связи необходимо развитие методов оценки трещиностойкости среды с неоднородной структурой. В работе трещиностойкость крупных поковок из улучшаемой стали 38ХН3МФА-Ш (0,38%C–Cr–3%Ni–Mo–V) определяли на основе критического раскрытия трещины δ_c и *J*-интеграла. Наличие критических этапов в развитии вязкой трещины при испытании оценивали по измерениям акустической эмиссии. В сочетании с полученными методами цифровой фрактографии 3D-изображениями изломов это позволило привязать форму и положение переднего фронта каждого скачка трещины к диаграмме «нагрузка – смещение». Измерение геометрии раскрытия трещины в процессе испытания показало возможность прямого определения коэффициента вращения берегов трещины при оценке δ_c. В целом это позволило построить карту распределения значений параметра δ_c по толщине образца и оценить масштаб разброса трещиностойкости в пределах одного образца – до 30 %. Такая локализация измерений, в первую очередь параметра δ_c, сопоставима с масштабом неоднородности строения морфологии различных типов структур, который был оценен на основе измерения цифровых изображений дендритной структуры, серного отпечатка по Бауману, неметаллических включений на нетравленом шлифе, феррито-перлитной полосчатости в микроструктуре. Это дает возможность для привязки локальных значений трещиностойкости к различным механизмам разрушения и сопутствующим им структурным составляющим.

Ключевые слова: неоднородность структур; трещиностойкость; акустическая эмиссия; фрактография; прогноз качества в металлургии; критическое раскрытие трещины; интеграл Черепанова – Райса; нелинейная механика разрушения.

Благодарности: Статья подготовлена по материалам докладов участников XI Международной школы «Физическое материаловедение» (ШФМ-2023), Тольятти, 11–15 сентября 2023 года.

Для цитирования: Сергеев М.И., Погорелов Е.В., Дударев А.А., Соколовская Э.А., Кудря А.В. О возможности локального измерения трещиностойкости конструкционных сталей с привязкой к структуре // Frontier Materials & Technologies. 2024. № 1. С. 71–81. DOI: 10.18323/2782-4039-2024-1-67-7.